J. Phys. F: Met. Phys. **18** (1988) 1299–1310. Printed in the UK

Amorphous yttrium–iron alloys: III. The influence of hydrogen

J M D Coey†, A Liénard‡, J P Rebouillat‡, D H Ryan§, Wang Zhenxi‖ and Yu Boliang†‖

† Department of Pure and Applied Physics, Trinity College, Dublin 2, Ireland
‡ Laboratorie Louis Néel, CNRS, 166X, 38042 Grenoble Cedex, France
§ Physics Department, McGill University, 3600 University Street, Montreal, Quebec H3A 2T8, Canada
‖ Institute of Physics, Chinese Academy of Sciences, Beijing, China

Received 21 July 1987, in final form 19 October 1987

Abstract. The effect of hydrogen on the magnetic properties of a series of sputtered $Y_{1-x}Fe_x$ alloys with $x = 0.32$, 0.48, 0.68, 0.82 and 0.88 is studied by magnetisation measurements and Mössbauer spectroscopy. Hydrogen desorption from all samples was followed by thermopiezic analysis. Dilation, x-ray and UV photoemission and low temperature specific heat were measured on iron-rich alloys ($x = 0.82$ or 0.88). All alloys except $x = 0.48$ absorb significant quantities of hydrogen (up to 4.5 moles per mole of yttrium). The added volume is $1.7\,cm^3mol^{-1}$. Photoemission spectra of hydrogenated iron-rich alloys resemble those of the crystallised material, having a large density of states at the Fermi level E_F and a specific heat coefficient γ of 13 mJ mol^{-1} K^{-2}; the density of states of the unhydrogenated material is much smaller although γ is larger. Magnetic order in the $x = 0.88$ sample evolves *continuously* from asperomagnetic to ferromagnetic with increasing hydrogen content; corresponding changes in magnetic ordering temperature, aligned moment in 5 T and total magnetic moment on the iron are from 109→525 K, 1.5→2.3 μ_B/Fe and 2.1→2.4 μ_B, respectively. The decrease in frozen spin disorder on hydrogenation is a consequence of a shift in the exchange distribution towards more positive values due to an increase in the average Fe–Fe distance and an increase in the density of states at E_F. The large linear specific heat and a linear temperature dependence of the average hyperfine field at low temperatures in the asperomagnetic state are linked to magnetic excitations of the frozen spin system. The critical concentration for the appearance of magnetism on the iron is reduced to $x \simeq 0.2$ on hydrogenation.

1. Introduction

The magnetic properties and Mössbauer spectra of a series of sputtered amorphous $Y_{1-x}Fe_x$ alloys with $0.32 \leqslant x \leqslant 0.88$ were described in two earlier papers (Coey *et al* 1981, Chappert *et al* 1981, hereafter referred to as I and II, respectively). It was found that a magnetic moment on the iron begins to develop when $x \geqslant 0.3$. As x increases, the average iron moment deduced from the ^{57}Fe hyperfine field distribution approaches 2.1 μ_B, although there is a wide range of composition where magnetic and non-magnetic iron sites coexist. In alloys with $x \geqslant 0.3$, magnetic ordering sets in below a temperature T_M, marked by a susceptibility maximum and the development of hysteresis. T_M increases with x to reach 109 K for $x = 0.88$ but the magnetic structure is

0305-4608/88/061299 + 12 $02.50 © 1988 IOP Publishing Ltd

not collinear for any composition, nor could the moment be fully aligned in applied fields of up to 18 T. Nevertheless there is evidence from the susceptibility above T_M (I) and inelastic neutron scattering below (Murani and Rebouillat 1982) that ferromagnetic correlations exist over a wide range of distances. The spin dynamics of the $x = 0.67$ composition resembles those of the dilute crystalline spin glass **Cu**Mn. Features that distinguish the iron-rich a-Y–Fe alloys from canonical spin glasses are the ease with which an appreciable fraction of the collinear saturation magnetisation can be induced by a small applied field, and the ferromagnetic hysteresis behaviour. The data can be rationalised by supposing that there is no long-range ferromagnetic component in zero field but that there are low-lying excited states where the iron moments are randomly orientated with *anisotropic* probability distribution to give a long-range ferromagnetic tic longitudinal component and randomly frozen transverse spin components; these are the asperomagnetic configurations, (Moorjani and Coey 1984) which possess a net moment (II). In zero field the correlation length or asperomagnetic 'domain' size is of order 25 Å (I).

The physical origin of the magnetic properties of a-Y–Fe was thought to be a distribution of Fe–Fe exchange interactions which is predominantly positive (ferromagnetic) but includes some negative (antiferromagnetic) coupling. This distribution was associated with the distribution of Fe–Fe nearest-neighbour distances present in the amorphous state (Forrester *et al* 1979), with negative exchange being associated with distances shorter than 2.54 Å. A ferromagnetic surface layer up to 3 nm thick with $T_c \sim 450$ K has been observed to form as the surface relaxes giving an increased average Fe–Fe distance (Bhagat and Lloyd 1981).

In order to test these ideas, we used hydrogen as a means of dilating the structure. Metallic glasses have a continuum of different absorption sites for hydrogen, and tend to form continuous solid solutions with hydrogen. In a preliminary report (Coey *et al* 1982) we found that the iron-rich alloys become good soft ferromagnets on hydrogenation, with Curie temperatures in excess of 400 K. An account of hydrogen uptake of melt-spun yttrium-rich compositions has appeared in recent conference proceedings (Coey *et al* 1985). Here we present a more extensive and quantitative report on the influence of hydrogen on a-$Y_{1-x}Fe_x$, including measurements not only of its effect on the sample volume, but also on the density of states detected by XPS and UPS. The magnetic properties are reported for a wide range of composition and hydrogen content.

2. Experimental results

Since the preparation and characterisation of the samples was fully described in I and II, it is sufficient here to give information on the hydrogenation procedure and characterisation of the hydrides, together with the main experimental results. Crystallisation temperatures, which were not included in I, were measured by differential scanning calorimetry (DSC); they are listed in table 1.

2.1. Preparation and characterisation

Samples for magnetisation and Mössbauer measurements were hydrogenated electrolytically using a current of order 1 mA mm^{-2} in a cell where the sample forms the cathode and the anode is a 100 mm^2 platinum electrode. In some cases the amorphous

Table 1. Characteristics of unhydrogenated and hydrogenated amorphous $Y_{1-x}Fe_x$ alloys.

Composition x	Hydrogen content y†	Crystallisation temperature T_x (K)	Magnetic ordering temperature T_M or T_c (K)	Hyperfine field $\langle B_{hf} \rangle$ (T)	Iron moment $\langle \mu_0 \rangle$‡	Iron moment $\langle \mu_2 \rangle$§
0.88	0.00	800	109(3)	30.1	2.08	1.51
	0.04		300(10)	—	—	1.90
	0.18		432(10)	—	—	2.20
	0.43		510(20)	33.7	2.32	2.32
	0.52		525(20)	34.5	2.40	2.32
0.82	0.00	770	108(3)	27.9	1.92	1.44
	0.67					
0.68	0.00	850	70(3)	24.5	1.69	1.11
	1.32					2.00
0.48	0.00	778	18(3)	8.8	0.61	0.42
0.32	0.00	726	—	0	0	0.15
	<0.72			5.0	0.31	

† An underestimate, since not all hydrogen is liberated at 1000 °C.
‡ Deduced from 4.2 K Mössbauer hyperfine field.
§ Measured in 5 T at 4.2 K.

Y–Fe foil was sandwiched between two sheets of stainless-steel mesh to avoid buckling and fracture. Several electrolytes were tried, but 0.1 M K_2CO_3 solution containing a trace of sodium arsenite was most satisfactory. It was noted that samples would absorb hydrogen from acid solutions without passing any current. Hydrogenation of the samples examined by photoemission in UHV was done by implantation *in situ*.

After hydrogenation, part of each foil was analysed by thermopiezic analysis (TPA) using an automated miniature thermomanometer specially designed for milligram samples (Ryan and Coey 1986). Masses used were in the 1–10 mg range and the maximum pressure of hydrogen evolved in the 2.68 cm^3 active volume of the device was 250 mbar (25 kPa). Data shown in figure 1 are expressed as pressure of hydrogen evolved per mg of yttrium, since iron is expected to play little part in the hydrogen uptake. The atomic ratio of hydrogen to yttrium is also given. The active volume was evacuated at room temperature before making the measurements by heating up to 1000 °C at a rate of 25 °C min^{-1}.

Iron-rich alloys ($x = 0.82$, 0.88) evolve as much as 4.5 H/Y on heating. These hydrogenated materials retain most of their hydrogen for periods of the order of a year at room temperature (Coey *et al* 1984). They are stable on heating up to above 100 °C in the thermopiezic analyser, but on further heating they lose hydrogen continuously up to their crystallisation temperature of about 500 °C, where the hydrogen pressure drops sharply. The likely explanation is that crystalline Y_2Fe_{17} or YFe_5 form hydrides which are stable to about 850 °C. On thermal recycling of the crystallised alloy in the analyser, the only hydrogen loss occurs near 850 °C. It is remarkable that the figure of 4.5 H/Y must be something of an *underestimate* of the hydrogen content of the starting amorphous alloy because hydrogen evolution is incomplete at 1000 °C.

Alloys richer in yttrium ($x<0.7$) evolve relatively little hydrogen when heated. Hydrogenated $Y_{0.32}Fe_{0.68}$ appears to be rather unstable; it shows significant hydrogen loss below 100 °C in the TPA curve of figure 1, and loses most of its hydrogen at room

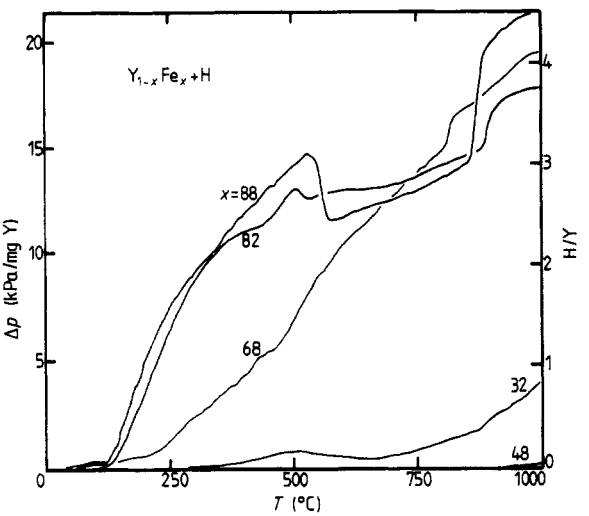

Figure 1. Thermopiezic analysis of hydrogenated amorphous Y–Fe alloys. The scales show the pressure of hydrogen evolved per mg of yttrium in the samples and the H/Y atomic ratio.

temperature in a matter of days. $Y_{0.52}Fe_{0.48}$ is worse in that hydrogen retention at room temperature is negligible. (No significant change was observed in Mössbauer isomer shift, nor is there any sign of hydrogen evolution by crystalline hydrides at the highest temperatures.) However, $Y_{0.68}Fe_{0.32}$ can be successfully hydrogenated and exhibits a drop in hydrogen pressure on crystallising to YFe_2+Y; the H/Y ratio in the hydrogenated amorphous alloy must be considerably greater than that measured because crystalline yttrium retains some hydrogen at temperatures well in excess of 1000 °C. It is clear from figure 1 that not all the hydrogen has been evolved at 1000 °C.

Figure 2 shows data which demonstrate that the alloys remain amorphous but expand on hydrogenation. The main maximum in the x-ray diffraction pattern moves inwards, corresponding to a dilation of approximately 2%. The increase in length of another sample measured at intervals during the course of hydrogenation saturates after about 20 minutes, at $\Delta l/l = 3.0(1)\%$. From this we can estimate the volume occupied by the hydrogen. Assuming a molar volume $\Omega = 9.5\,\text{cm}^3$ for $Y_{0.12}Fe_{0.88}$ ($\rho = 6.3\,\text{g cm}^{-3}$) based on the elemental liquid densities, the 3.0% linear expansion corresponds to a volume of $0.88\,\text{cm}^3\,\text{mol}^{-1}$. The composition of the fully hydrogenated alloy deduced from TPA is $Y_{0.12}Fe_{0.88}H_{0.52}$ so the added volume due to hydrogen is $\Delta V = 1.7\,\text{cm}^3\ \text{mol}^{-1}$ of H or $2.8\,\text{Å}^3$/H atom†. These values are in excellent agreement with those found in a wide range of crystalline alloys (Peisl 1978, Westlake 1983, Maeland 1985); $\Delta V/\Omega = 0.18$.

2.2. *Electronic structure*

The increase in Mössbauer isomer shift δ on hydrogenation of aY–Fe has been fully described in another paper (Coey *et al* 1984). The effect for $Y_{0.12}Fe_{0.88}$, $(\partial\delta/\partial \ln V) = -2.5\,\text{mm s}^{-1}$, is about twice as large as the volume dependence of the isomer shift that

† A much smaller value (0.5 Å^3/atom) was quoted earlier because of an error in calculation (Coey *et al* 1984).

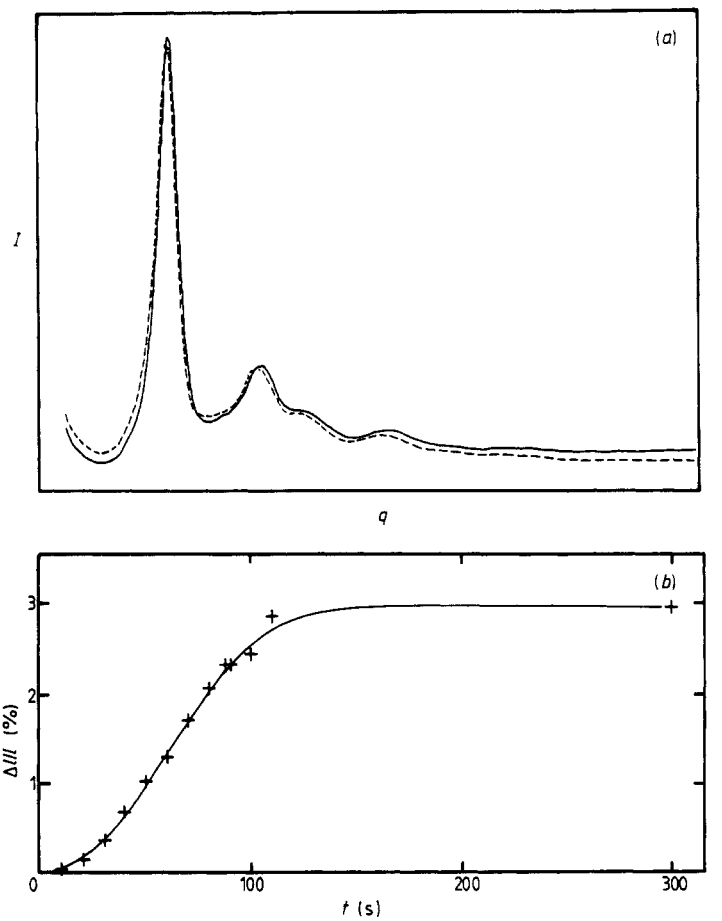

Figure 2. Dilation of amorphous Y–Fe on hydrogenation. (*a*) X-ray diffraction trace of $Y_{0.32}Fe_{0.68}$ before (full curve) and after (broken curve) hydrogenation. (*b*) Expansion of $Y_{0.12}Fe_{0.88}$ as a function of hydrogenation time.

would normally be expected (Kalvius *et al* 1974). It appears that there must be a significant modification of the electronic structure by hydrogen.

To investigate this point further we have carried out UPS and XPS measurements on the $Y_{0.18}Fe_{0.82}$ alloy in the amorphous, hydrogenated and crystallised states. A VG system with double anode (Al/Mg) operating in a vacuum of 5×10^{-10} Torr was used, and the surface was cleaned by argon-ion bombardment at 5–10 min intervals. No Ar peak was observed, and there was only a slight trace of O 2s at -531.6 eV. The Fermi energy was defined by a Ni standard. The changes of state were followed *in situ* by proton bombardment or heating the amorphous starting alloy. Figure 3 compares UPS data with the sample at 300 °C and 600 °C. The same broad spectrum is observed throughout the range 25–500 °C, but on crystallisation at 600 °C it changes completely to show a large increase in density of states near the Fermi level E_F due to the iron 3d bands. The spectra of the hydrogenated and crystallised films are similar, except for the presence of a peak at 11 eV in the former case which may be associated with hydrogen-like states.

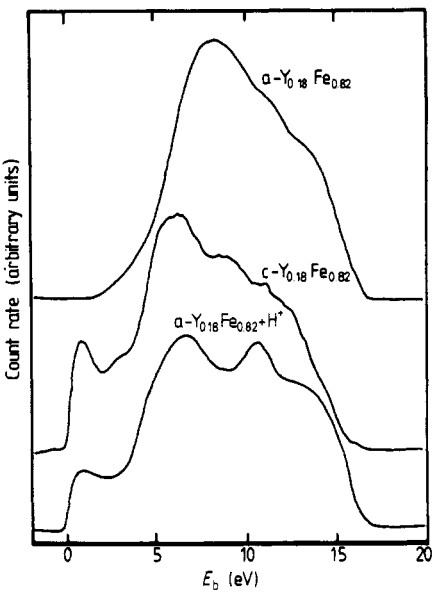

Figure 3. UPS spectra of $Y_{0.18}Fe_{0.82}$ in the amorphous, hydrogenated amorphous and crystallised states.

XPS data in figure 4 confirm the resemblance between the crystallised and hydrogenated states. The amorphous alloy at 500 °C, before crystallisation, shows a flat density of states which drops off 1 eV below E_F. After crystallisation or hydrogenation the density of states near E_F becomes much larger. This fits in with the observation that the isomer shifts of iron-rich hydrogenated amorphous alloys approach those of the ferromagnetic crystalline Y–Fe phases.

Another measurement which is sensitive to the density of states at E_F is the low-temperature specific heat. We have examined amorphous $Y_{0.12}Fe_{0.88}$ before and after hydrogenation. Milligram samples were measured using the thermal relaxation

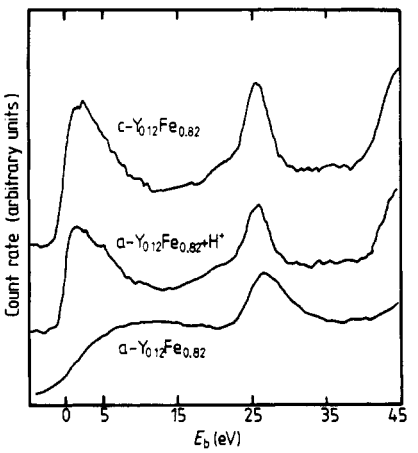

Figure 4. XPS spectra of $Y_{0.18}Fe_{0.82}$ in the amorphous, amorphous hydrogenated and crystallised states.

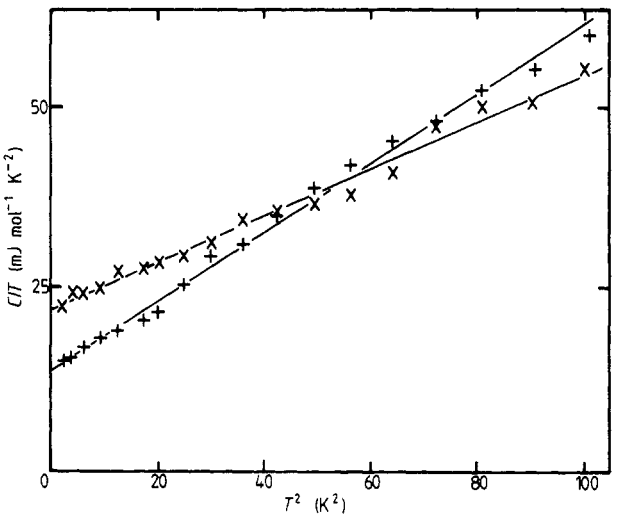

Figure 5. Low temperature specific heat of amorphous $Y_{0.12}Fe_{0.88}$ before (×) and after (+) hydrogenation.

method (Backmann *et al* 1972) in an apparatus constructed by R Buder. Normally, the low temperature specific heat of a metal can be represented by the expression $C=\gamma T+\beta T^3$; results are plotted in figure 5 as $C/T:T^2$. γ is 23(1) mJ mol^{-1}K^{-2} and it cannot be mainly electronic in origin, since the density of states at the Fermi level (figures 3 and 4) is too small to account for the large value of γ observed, and increases sharply on hydrogenation while γ actually falls to 13(1) mJ mol^{-1} K^{-2}. β is 0.33 and 0.48 mJ mol^{-1} K^{-4} in the two cases, corresponding to Debye temperatures of 181 K and 159 K for the unhydrogenated and hydrogenated materials respectively.

2.3. *Magnetic properties*

Hydrogenation completely changes the nature of the magnetic order in the iron-rich alloys. This is apparent from the 4.2 K magnetisation curves shown in figure 6. Before

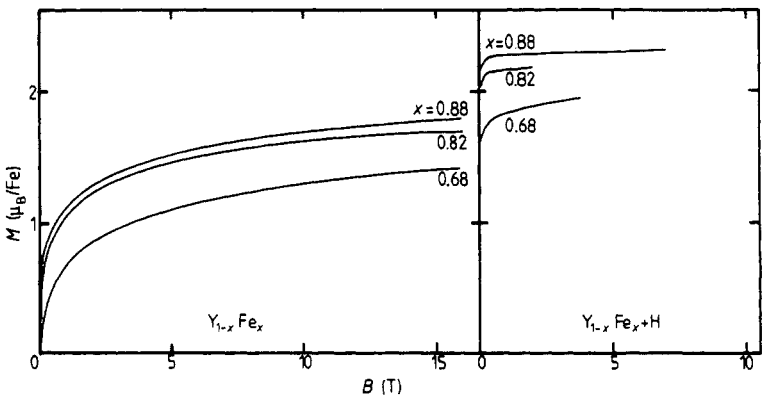

Figure 6. Magnetisation curves at 4.2 K for amorphous $Y_{1-x}Fe_x$ alloys with $x=0.68$, 0.82 and 0.88 before and after hydrogenation.

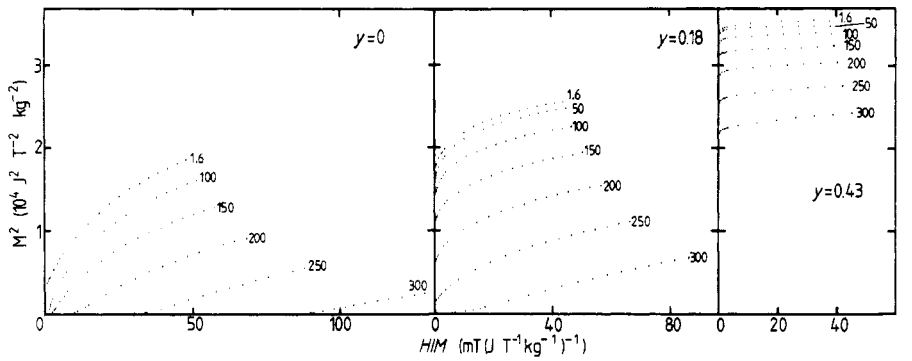

Figure 7. Arrott plots for $Y_{0.12}Fe_{0.88}$ with different hydrogen contents. The curves are labelled with their T (K) values.

hydrogenation, alloys have a noncollinear magnetic structure and the magnetisation of the iron-rich alloys approaches saturation as log H (i.e. $dH/dM \propto H$ at any temperature). This law will be discussed elsewhere. However, on saturation with hydrogen both $x = 0.82$ and 0.88 alloys become collinear ferromagnets, and the $x = 0.63$ alloy is nearly so. Ferromagnetic saturation moments after hydrogenation are a little in excess of $2\mu_B$, in agreement with moments deduced from the average hyperfine field (table 1).

In order to follow the evolution of the magnetic structure as a function of hydrogen content y we have examined the $Y_{0.12}Fe_{0.88}H_y$ alloy in some detail; electrolysis was arrested before saturation, magnetisation curves were obtained as a function of temperature from 1.6 K to 300 K and the same sample was then loaded with more hydrogen and remeasured. There were four electrolysis steps covering the range $0 \leqslant y \leqslant 0.52$. Continuous evolution towards a ferromagnetic state occurs with increasing y; the saturation magnetisation deduced from Arrott plots increases, while the high field slope decreases. Some of the Arrott plots are illustrated in figure 7, and magnetisation curves obtained at 4.2 K in decreasing field are shown in figure 8.

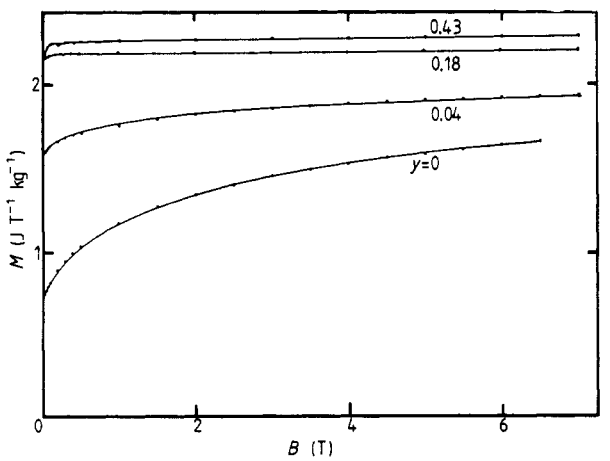

Figure 8. Magnetisation curves at 4.2 K for $Y_{0.12}Fe_{0.88}$ as a function of hydrogen content y.

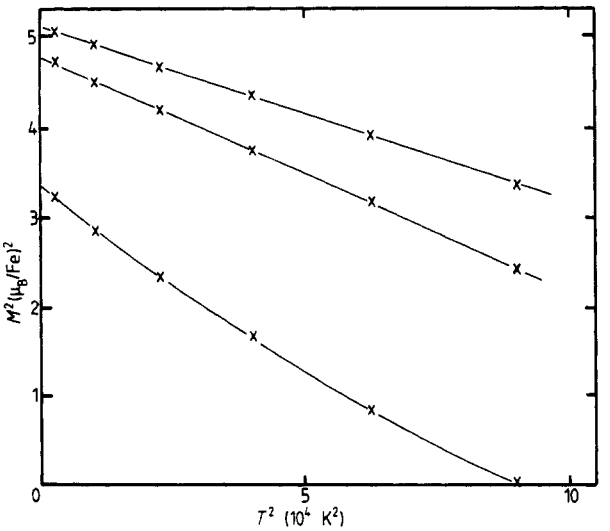

Figure 9. M^2:T^2 plot for $Y_{0.12}Fe_{0.88}$ with varying amounts of hydrogen.

The temperature variation of the zero-field magnetisation extrapolated from the Arrott plots can be represented by straight lines on an M^2:T^2 diagram for the larger values of hydrogen content. Similar behaviour has been observed previously in amorphous Y–Ni alloys without hydrogen (Liénard and Rebouillat 1978). It is by extrapolating the data in figure 9 that we deduce the value of T_c for the alloys with $y>0.1$, which cannot be measured directly because hydrogen loss becomes important above $\simeq 100$ °C.

2.4. Mössbauer spectra

The Mössbauer spectra of unhydrogenated amorphous $Y_{1-x}Fe_x$ have been discussed in detail in II. The $Y_{0.12}Fe_{0.88}$ sample shows a distribution of hyperfine field, which remains broad after hydrogenation but with an increased average value. Average iron moments in table 1 are deduced from the average 4.2 K hyperfine fields using the conversion of 14.5 T/μ_B discussed previously.

In the case of $Y_{0.68}Fe_{0.32}$ alloy, we established in II that this was nonmagnetic at 4.2 K with no moment on the iron. The iron content was below the critical concentration x_c for the appearance of magnetism. On hydrogenation, the quadrupole doublet is broadened at 4.2 K and there appears a clear hyperfine splitting for about 30% of the iron. The critical concentration is shifted to lower values of x in sputtered, as it is in melt-spun yttrium-rich Y–Fe amorphous alloys (Ryan *et al* 1985). The shift in x_c is estimated to be about 0.10.

3. Discussion

The dramatic transformation of the iron-rich alloys from asperomagnets with a spin freezing temperature near 100 K to ferromagnets with a Curie point of up to 500 K is attributed to a hydrogen-induced shift in the distribution of exchange interactions

towards more positive values. This was originally related to the dilation of the noncrystalline lattice (Coey *et al* 1982), but it is now clear that a change in structure of the 3d band, evident from photoemission, will also play a part. We reject the hypothesis that the noncollinear structures could be due to random-site anisotropy related to an orbital contribution to the 3d moment, because of the hydrogen-induced ferromagnetism of the iron alloy, and the fact that the corresponding cobalt and nickel alloys are already good ferromagnets (Heiman and Kazama 1978, Liénard and Rebouillat 1978).

The dilation explanation for the change in magnetic properties is based on analogy with the behaviour of FCC iron. Some structural resemblances have been detected between iron-rich amorphous alloys and FCC iron (Cowlam and Carr 1985), particularly concerning nearest-neighbour distances and coordination number. The work of Gradmann and collaborators with epitaxially-grown FCC iron layers on copper (Kümmerle and Gradmann 1977), and other work on FCC iron precipitates in copper (Johanson *et al* 1970) has established the change in sign of the iron–iron interaction from negative for $d_{FeFe}<2.54$ Å to positive for $d_{FeFe}>2.54$ Å.

The change in d-band structure near E_F evident in figures 3 and 4 when the iron-rich amorphous alloy is hydrogenated or crystallises is quite remarkable. It seems unlikely that the lack of d states near E_F in the amorphous alloy is an experimental artefact or due to surface contamination because the change is observed between 500 °C and 600 °C which is precisely where a-$Y_{0.18}Fe_{0.82}$ crystallises. Extensive photoemission work on amorphous Cu–Zr alloys has shown that there is stabilisation of the 3d bands by about 1 eV in the amorphous state (Oelhaven 1983). However, an earlier x-ray photoemission study of a-$Y_{0.21}Fe_{0.79}$ by Connell *et al* (1984) found a sharp peak in the density of states at E_F, similar to our results on crystallised or hydrogenated material.

The large 3d density of states at E_F in the hydrogenated, ferromagnetic form of a-Y–Fe is consistent with the large linear specific heat ($\gamma = 13$ mJ mol^{-1} K^{-2}), and it may also be related to the increase in iron moment (table 1) and the change from asperomagnetic to ferromagnetic order. The iron moment could be regarded as the sum of a contribution of about $2\,\mu_B$ in relatively narrow, and localised d levels, plus an extra contribution due to Stoner-type band splitting, which also enhances the ferromagnetic coupling. The latter term is about $0.3\,\mu_B$ in the hydrogenated alloys, but it is negligible in unhydrogenated a-Y–Fe due to its much lower density of states. An increase of $0.3\,\mu_B$ on hydrogenation is also found in a-Sc–Fe(unpublished), a-Zr–Fe (Ryan *et al* 1987a) and a-Hf–Fe (Ryan *et al* 1987b) alloys. It is clear from our data that the magnetic moment of iron does not collapse when it ceases to be a collinear ferromagnet.

Besides the increase in moment, enhancement of the Curie temperature by hydrogen is also observed in the other iron-rich amorphous alloys Zr–Fe (Fujimori *et al* 1984, Ryan *et al* 1987a), Hf–Fe (Ryan *et al* 1987a, b) and Sc–Fe (unpublished). The Sc–Fe system exhibits similar magnetic properties to Y–Fe, although the iron moment is smaller ($1.6\,\mu_B$) (Day *et al* 1985). However, the Zr and Hf data differ from iron-rich amorphous Y–Fe (the comparison is being made in the unhydrogenated state) in that they are closer to ferromagnetism than the Y material. They show a double magnetic transition with increasing temperature passing first from asperomagnets to wandering-axis ferromagnets at T_{xy}, and then to paramagnets at T_c. The frozen transverse spin components therefore unblock at a different temperature to the longitudinal component in a-Zr–Fe and a-Hf–Fe, whereas there is a single spin freezing temperature for

a-Y–Fe. In a-$Zr_{0.09}Fe_{0.91}$, the ferromagnetic correlation length is found to be 23 Å and essentially independent of temperature below T_c (Rhyne and Fish 1985). A similar value was estimated in I for a-$Y_{0.32}Fe_{0.68}$.

An important result, deduced from our data on the $x = 0.88$ sample at 4.2 K as a function of hydrogen content, is that there is apparently no abrupt change in the magnetic ground state as the exchange distribution is shifted towards more positive values. In a given field, the moment increases steadily with y, and the magnetisation curves approach saturation more readily as the asperomagnetic order evolves *continuously* towards collinear ferromagnetism. We do not appear to cross any spin-glass–ferromagnetic phase boundary at $T = 0$.

The exceptionally large linear specific heat of the unhydrogenated a-$Y_{0.12}Fe_{0.88}$ alloy ($y = 23$ mJ mol^{-1} K^{-2}) is unlikely to be electronic in origin in view of the small density of states at E_F found by photoemission. Large linear terms have also been reported in the a-Zr–Fe (Mizutani *et al* 1984) and a-Hf–Fe (Ryan *et al* 1987b) systems, for which a near-linear variation of average hyperfine field with temperature is also found (Ryan *et al* 1987a) (this behaviour in a-Y–Fe was already remarked upon in II). It is tempting to attribute both effects to excitations of transverse spin components which would have to follow a dispersion relation $E \propto k^3$, as for a two-dimensional ferromagnet.

Finally, the influence of hydrogen on the appearance of magnetism was studied previously in some detail for melt-spun a-Y–Fe ribbons with $x \simeq 0.35$ (Ryan *et al* 1985). Here we find a similar effect in sputtered a-$Y_{0.68}Fe_{0.32}$. This composition is nonmagnetic without hydrogen (II), but an iron moment of order 0.3 μ_B has developed on about 40% of the iron sites after hydrogenation. The Y→H electron transfer may reduce the Y–Fe hybridisation sufficiently to allow a moment to appear on iron sites with four or more iron neighbours (as opposed to six or more without hydrogen (II)). It is interesting that a moment on the iron is found to develop inhomogeneously on hydrogenating *crystalline* Hf_2Fe (Vulliet *et al* 1984) so that even in the saturated alloy magnetic and nonmagnetic iron atoms coexist.

4. Conclusions

Our work on the hydrogenated amorphous $Y_{1-x}Fe_x$ system leads us to conclude:

(i) substantial amounts of hydrogen can be introduced into the amorphous alloys, except when $x \simeq 0.5$;

(ii) the volume occupied by absorbed hydrogen is 1.7 cm^3 mol^{-1}, as in many crystalline materials;

(iii) the asperomagnetic→ferromagnetic transformation induced by hydrogen in the iron-rich alloys is due to a modification of the Fe–Fe exchange distribution towards more ferromagnetic values. The change is related to dilation of the average Fe–Fe distances and a substantial increase in the electronic density of states near E_F;

(iv) the modification of the magnetic structure appears to be continuous as a function of hydrogen content;

(vi) there is a shift in the critical concentration for the appearance of magnetism with hydrogen from $x \simeq 0.3$ to $x \simeq 0.2$.

Acknowledgments

This work was completed while one of the authors (JMDC) was Collaborateur Temporaire Etranger at the Centre d'Etudes Nucléaires de Grenoble and another (JPR) was at the Institute of Physics (Beijing) in the framework of the CNRS–Academia Sinica Exchange Programme. Experimental help from R Buder, K Donnelly and M Kabsch is gratefully acknowledged. The work was supported in part by the Commission of the European Communities under contract no SUM-041-EIR.

References

Backmann R, DiSalvo F J, Geballe T H, Greene R L, Howard R E, King C N, Kirsch H C, Lee K N, Schwall R E, Thomas H-U and Zubeck R B 1972 *Rev. Sci. Instrum.* **43** 205–10

Bhagat S M and Lloyd J N 1981 *J. Appl. Phys.* **52** 1838–40

Chappert J, Coey J M D, Liénard A and Rebouillat J P 1981 *J. Phys. F: Met. Phys.* **11** 2727–44

Coey J M D, Givord D, Liénard A and Rebouillat J P 1981 *J. Phys. F: Met. Phys.* **11** 2707–25

Coey J M D, Ryan D H, Altounian Z, Maris P and Ström-Olsen J O 1985 *Rapidly Quenched Metals* ed. S Steeb and H Warlimont (Amsterdam: Elsevier) pp 1573–6

Coey J M D, Ryan D H, Gignoux D, Liénard A and Rebouillat J P 1982 *J. Appl. Phys.* **53** 7804–6

Coey J M D, Ryan D H and Yu Boliang 1984 *J. Appl. Phys.* **55** 1800–4

Connell G A N, Oh S J, Allen J and Allen R 1984 *J. Non-Cryst. Solids* **61–62** 1061–6

Cowlam N and Carr G E 1985 *J. Phys. F: Met. Phys.* **15** 1109–16, 1117–26

Day R K, Dunlop J B, Foley C P, Ghafari M and Pask H 1985 *Solid State Commun.* **56** 843–6

Forrester D W, Koon N C, Schelleng J H and Rhyne J J 1979 *Solid State Commun.* **30** 177–80

Fujimori H, Nakanishi H, Hirsyoshi H and Kazama N S 1982 *J. Appl. Phys.* **53** 7792–4

Gabay M and Toulouse G 1981 *Phys. Rev. Lett.* **47** 201–4.

Heiman N and Kazama N 1978 *Phys. Rev.* B **17** 2215–22

Johanson G J, McGirr M B and Wheeler D A 1970 *Phys. Rev.* B **1** 3208

Kalvius G M, Klein V F and Wortmann G 1974 *J. Physique* **35** 139–49

Kümmerle W and Gradmann U 1977 *Solid State Commun.* **24** 33–6

Liénard A and Rebouillat J P 1978 *J. Appl. Phys.* **49** 1680–3

Maeland A J 1985 *Rapidly Quenched Metals* ed. S Steeb and H Warlimont (Amsterdam: Elsevier) pp 1507–14

Mizutani V, Matsuura M and Fukamichi K 1984 *J. Phys. F: Met. Phys.* **14** 731–8

Moorjani K and Coey J M D 1984 *Magnetic Glasses* (Amsterdam: Elsevier) ch 1, pp 31–6

Murani A P and Rebouillat J P 1982 *J. Appl. Phys.* **55** 1800–4

Oelhaven P 1983 *Glassy Metals II* ed. H Beck and H-J Guntherodt (Berlin: Springer) pp 283–323

Peisl H 1978 *Hydrogen in Metals I* ed. G Alefeld and J Volkl (Berlin: Springer) pp 53–74

Rhyne J J and Fish G E 1985 *J. Appl. Phys.* **57** 3407–10

Ryan D H, Cadogan J M, Devlin E J and Coey J M D 1985 *Z. Phys. Chem.* **145** 113–20

Ryan D H and Coey J M D 1986 *J. Phys. E: Sci. Instrum.* **19** 693–4

Ryan D H, Coey J M D, Batalla E, Altounian Z and Ström-Olsen J O 1987a *Phys. Rev.* B **35** 8630–8

Ryan D H, Coey J M D and Ström-Olsen J O 1987b *J. Magn. Magn. Mater.* **67** 148–54

Vulliet P, Teisseron G, Oddou J L, Jeandey C and Yaouanc A 1984 *J. Less-Commom Met.* **104** 13–20

Westlake D G 1983 *J. Less-Common Met.* **90** 251–75